

# Large dielectrophoresis force and torque induced by localized surface plasmon resonance of Au nanoparticle array

Xiaoyu Miao and Lih Y. Lin

Electrical Engineering Department, University of Washington, Seattle 98195, USA

Received September 8, 2006; revised October 19, 2006; accepted October 20, 2006;  
posted October 24, 2006 (Doc. ID 74895); published January 12, 2007

A new approach is proposed for manipulating and rotating micro- or nano-objects by using polarized laser light with low intensity. The polarized light excites resonant dipoles on a cap-shaped Au nanoparticle array, which generates a highly nonuniform radiation field that induces large dielectrophoresis force on dielectric objects. The orientation control of the objects is realized by adjusting the polarization direction of the incident light. Theoretical modeling, fabrication, and characterization results for the cap-shaped Au nanoparticle array, as well as preliminary trapping results, are reported. © 2007 Optical Society of America  
OCIS codes: 240.6680, 260.3910, 140.7010.

Noninvasive manipulation of micro- or nano-objects is an important tool for basic biological research. It allows cells and cellular components treated with biochemical tags to be collected, separated, concentrated, and transported without damage to the objects themselves. In the past, dielectrophoresis has been the most widely employed method for such purposes.<sup>1</sup> Recently, achieving such a goal by using light has attracted much attention, since the location of exerted force not only can be precisely defined, but also is flexible and can be controlled by scanning the light. The concept of optical tweezers that utilizes radiation pressure from photons was first proposed to realize this.<sup>2</sup> The disadvantage of optical tweezers lies in the high optical intensity needed to generate enough force.<sup>3</sup> Recently, optoelectronic tweezers was proposed to reduce the intensity requirement in optical manipulation.<sup>4</sup> Among various noninvasive manipulation mechanisms, a particularly desirable one is to control the orientation of the objects, in addition to trapping and moving them. Such capability opens the door to building structured biomaterials for potential applications in constructing biofilms and in human tissue engineering. Conventional optical tweezers can trap and move the objects around by attraction or repulsion, but without the capability to control object orientation. The DEP and electrorotation technologies can achieve such control. However, such systems consist of fixed electrodes used to generate the electric field; therefore, they lose the advantages possessed by the optical methods described above. Furthermore, the resolution of orientation control is coarse, and the methods are limited in area for bioconstruction and manipulation.

This Letter shows that trapping and rotation can be realized through DEP generated by the radiation field from light-induced oscillating dipoles on the surface of metal nanoparticles. The chief advantages of this approach are a fine orientation control ability and a low optical intensity requirement. Figure 1 illustrates the working principle of the approach. Polarized light induces a localized surface plasmon resonance on the surface of a Au nanoparticle array.

The surface plasmon consists of resonant dipole moments that radiate and create a patterned radiation field with a large gradient in the liquid solution. A large DEP force can be induced on the dielectric objects inside the solution without requiring high optical intensity. Changing the polarization of the incident light can change the radiation pattern, thus achieving fine orientation control of the objects. The incident light has an electric field component  $\mathbf{E}_0$ . The magnitude of the electric field is related to the intensity of the focused light  $I$  by  $E_0 = (2\eta_1 I)^{1/2}$ , where  $\eta_1$  is the impedance of the liquid solution. By solving the induced motion of oscillating electrons under this electric field, the total dipole moment of the oscillating dipoles can be described by<sup>5</sup>

$$P = \int A n d p = \frac{4A n q^2 n_1}{m \omega \alpha \sqrt{n_1^2 \omega^2 + \omega_p^2 - \omega^2}} E_0, \quad (1)$$

where  $q$  and  $m$  are the charge and the mass of a single electron, respectively,  $n_1$  is the refractive index

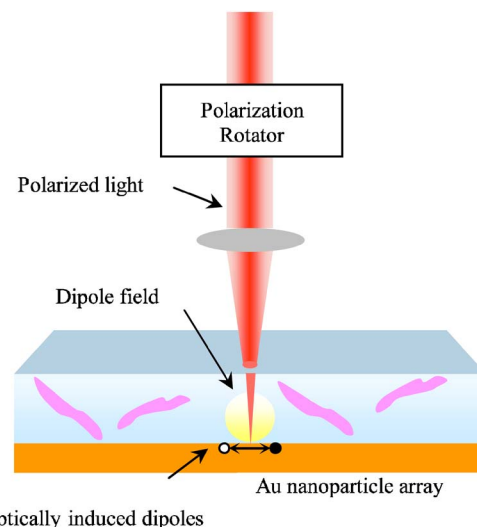


Fig. 1. (Color online) Manipulating and rotating biological cells with polarized light.

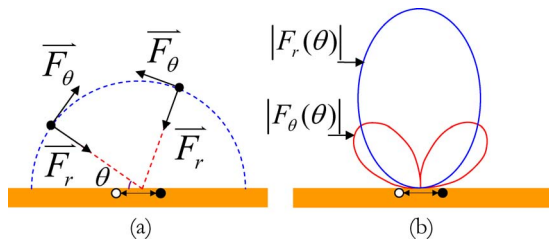


Fig. 2. (Color online) (a) Direction of the radial force and angular force component; (b) amplitude cross section of the radial force and angular force. The distance between a point on the curve and the dipole center represents the force amplitude at that orientation.

of the solution,  $\omega$  is the angular frequency of the incident light,  $\omega_p$  is the plasma frequency of bulk Au,  $\alpha$  is the attenuation coefficient of the incident light in Au,  $A$  is the area of the light spot, assuming uniform intensity, and  $n$  is the free-electron density of Au. The resonant dipoles are known as Hertzian dipoles, with their magnitude much smaller than the wavelength of the radiation field. The direction of the dipoles is parallel to the electric field polarization of the incident light. They radiate and create a patterned radiation field, which is approximated by<sup>6</sup>

$$E = \frac{k^2 P}{4\pi\epsilon_1 r} \sin\theta \exp i\omega(t - r/c), \quad (2)$$

where  $k$  is the wavenumber,  $\epsilon_1$  is the dielectric constant of the liquid solution,  $r$  is the radial distance from the center of the light spot, and  $\theta$  is the longitudinal angle from the dipole axis. The DEP force induced by the nonuniform field  $E$  on a dielectric spherical object is given by  $\mathbf{F}_{\text{DEP}} = 2\pi R^3 \epsilon_1 K^{(1)} \nabla E^2$ , where  $R$  is the radius of the object and  $K^{(1)}$  is the Clausius–Mossotti factor.<sup>1</sup> Substituting Eq. (2) into this general expression, the DEP force induced by the radiation field becomes

$$\mathbf{F} = 2\pi R^3 \epsilon_1 K^{(1)} \left( \frac{k^2 P}{4\pi\epsilon_1} \right)^2 \left( -\hat{r} \frac{2}{r^3} \sin^2\theta + \hat{\theta} \frac{2}{r^3} \sin\theta \cos\theta \right) \equiv F_r \hat{r} + F_\theta \hat{\theta}. \quad (3)$$

As shown in Eq. (3), the light-induced DEP force consists of two components: radial force  $F_r$  and angular force  $F_\theta$ . Figures 2(a) and 2(b) show the direction and amplitude cross section of the two force components, respectively. The combined effect of the radial force and angular force will pull the object toward the angular force valley at the  $\theta = 90^\circ$  equator and align the long axis of the object orthogonal to the polarization direction of the incident light. Since the polarization can be tuned very precisely, fine orientation control can be achieved.

A *Listeria* cell, an intracellular bacteria pathogen elliptical in shape, is used as an example to model the light-induced DEP force and associated torque. The radii of the long axis and short axis of the cell are 0.65 and 0.2  $\mu\text{m}$ , respectively. A shell model is used to represent the equivalent dielectric constant of the

whole cell.<sup>7</sup> By partitioning the elliptical cell into an array of spherical components 10 nm in diameter, the light-induced DEP force can be calculated by using Eq. (3). Figure 3(a) shows the maximum light-induced DEP force exerted on the cell as a function of vertical distance from the Au nanoparticle array under different light intensities. The modeling results suggest that a force  $\sim 1$  pN can be achieved at a radial distance of 1  $\mu\text{m}$  with an incident light power as small as 0.1 mW focused into a 100  $\mu\text{m}^2$  spot. Such intensity is much lower than the requirement for conventional optical tweezers. The associated torque exerted on the cell is plotted as a function of time in Fig. 3(b), assuming that the cell's long axis is oriented at  $45^\circ$  with respect to light polarization initially, and the viscosity of the liquid solution is  $8.9 \times 10^{-4}$  Pa s. The inset shows the rotation trajectory of the cell. The result confirms that the long axis of the cell will be aligned to the direction orthogonal to the polarization of the incident light, as discussed earlier in the force analysis.

Au nanoparticle array is chosen as a platform for the surface plasmon resonance instead of Au film. This is because the resonant wavelength of the Au nanoparticle is tunable and can be designed for longer wavelength, which is more biocompatible. Furthermore, unlike conventional surface plasmon resonance in metal thin films, the light's incident angle does not need to be precisely controlled, and the induced surface plasmon is localized. The Au nanoparticles are formed by evaporating a thin layer of Au on a self-assembled polystyrene sphere monolayer.<sup>8</sup> Figures 4(a) and 4(b) show the scanning electron micrograph of the structures formed by us-

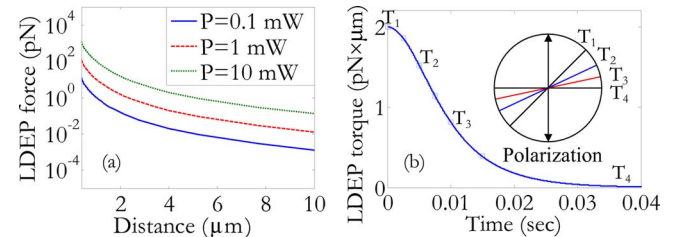


Fig. 3. (Color online) (a) Induced DEP force exerted on the cell versus the vertical distance from the Au nanoparticle array under various incident light power; (b) associated torque exerted on the cell versus time. The inset shows the corresponding rotation trajectory for the cell's long axis.

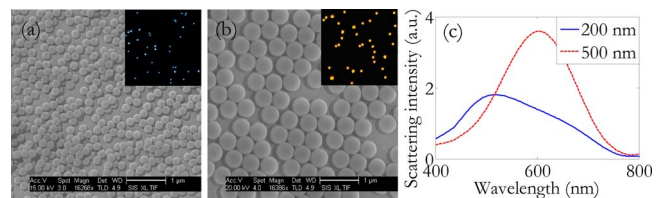


Fig. 4. (Color online) Scanning electron micrograph of the cap-shaped Au nanoparticle array. (a) Sample formed with 200 nm polystyrene spheres; (b) sample formed with 500 nm polystyrene spheres; (c) scattering spectra of the Au nanoparticle array formed with 200 and 500 nm polystyrene spheres. The insets in (a) and (b) are the corresponding dark-field fluorescence microscope images taken at regions with sparse distribution.

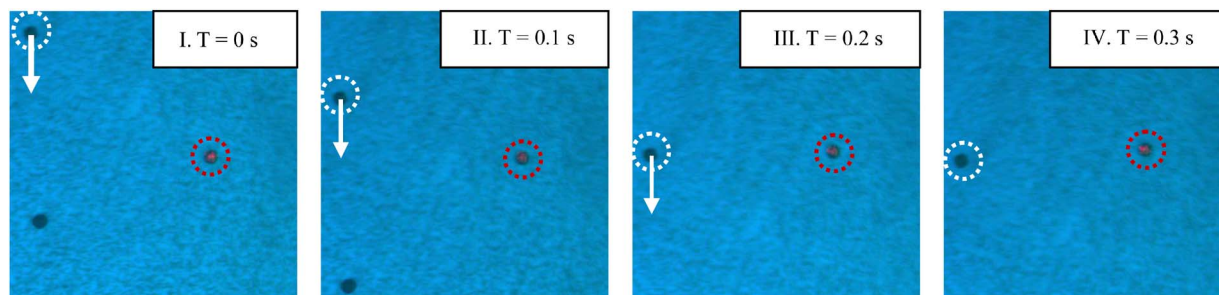


Fig. 5. (Color online) Demonstration of trapping a single polystyrene sphere by using the proposed approach. The polystyrene sphere located at the light spot (circled in black or red) is trapped, while other polystyrene spheres (circled in white) in the suspension move together with the motorized stage.

ing polystyrene spheres with different sizes. The insets are the fluorescence optical microscope images under dark-field illumination. The scattering light represents the radiation field generated by the oscillating dipoles. Nanoparticles with different sizes show different scattering resonant wavelengths. The scattering spectra of the samples are measured by collecting the scattering light under dark-field illumination and then characterized by using a UV-visible spectrometer. The results are shown in Fig. 4(c). The results indicate that the cap-shaped Au nanoparticle array formed with larger polystyrene spheres has a longer scattering resonant wavelength and higher scattering efficiency. In the previous discussion on modeling, the external scattering efficiency is assumed to be 100%. In other words, all input optical power is assumed to be converted to surface plasmon energy, and the oscillating dipoles are assumed to decay completely through radiative damping. However, part of the input light will be reflected, and nonradiative decay mechanisms also exist in these nanoparticles. We characterize this by defining the external scattering efficiency as the ratio between the power of the light scattered through localized surface plasmon resonance and the power of the incident light at the resonance peak. The experimental results based on the spectral measurement give an external scattering efficiency of 6.39% and 22.78% for the fabricated cap-shaped Au nanoparticle arrays formed with 200 and 500 nm polystyrene spheres, respectively. This means that the power of the laser source used in the experiment needs to be  $\sim 4.4$  times larger than the theoretical value that assumes 100% scattering efficiency for the same force, for the cap-shaped Au nanoparticle array formed with 500 nm polystyrene spheres. This is still lower than what is required for conventional optical tweezers. The scattering efficiency can be increased by improving the density of the Au nanoparticle arrays, as well as by tuning the diameters of the polystyrene spheres and the thickness of the Au coating.

To demonstrate the trapping capability of the proposed approach, a drop of diluted polystyrene sphere ( $10\ \mu\text{m}$  in diameter) suspension with volume  $1\ \mu\text{l}$  is added on the surface of the sample shown in Fig. 4(b). An epi-illumination fluorescence microscope

(AXIO Imager DI from Zeiss) is adopted as the observation platform. A He-Ne laser with the wavelength  $\lambda = 633\ \text{nm}$  is coupled into the optical path of the microscope, by using the periscope assembly setup, to excite the resonance on the Au nanoparticles. The minimum optical power needed to induce the trapping measured under the objective lens of the microscope is  $\sim 1.0\ \text{mW}$ . The area of the focused light spot on the Au nanoparticle array is about  $300\ \mu\text{m}^2$ . The trapping effect is demonstrated in Fig. 5, where the motorized stage and therefore the other polystyrene spheres are moved relative to the trapped sphere. Further experimental work to demonstrate the capability of fine orientation control is underway.

In conclusion, a new approach for optical manipulation and rotation of micro- or nano-objects with fine orientation control has been proposed. The fabrication results show that the cap-shaped Au nanoparticle array can achieve adequate scattering efficiency through localized surface plasmon resonance. Trapping the polystyrene sphere by using the proposed approach is also realized.

This project is supported by the National Science Foundation (DBI 0454324) and the National Institutes of Health (1 R21 EB005183). The authors thank Suzie Pun and Younan Xia for valuable discussions. X. Miao's e-mail address is xiaoyu@ee.washington.edu.

## References

1. T. B. Jones, *Electromechanics of Particles* (Cambridge U. Press, 1995).
2. A. Ashkin, Proc. Natl. Acad. Sci. USA **94**, 4853 (1997).
3. K. C. Neuman, E. H. Chadd, G. F. Liou, K. Bergman, and S. M. Block, Biophys. J. **77**, 2856 (1999).
4. P. C. Chiou, A. T. Ohta, and M. C. Wu, Nature **436**, 370 (2005).
5. X. Miao, "Opto-plasmonic tweezers for manipulation and rotation of micro/nano objects—design and fabrication," Masters thesis (University of Washington, Seattle, 2006).
6. J. D. Jackson, *Classical Electrodynamics* (Wiley, 1975).
7. M. Nishioka, S. Katsura, K. Hirano, and A. Mizuno, IEEE Trans. Ind. Appl. **33**, 1381 (1997).
8. X. Miao, H. Liao, and L. Y. Lin, in *Proceedings of IEEE International Conference on Optical MEMS and Their Applications* (IEEE, 2005), pp. 15–16.